Ξ_{bb} and Ω_{bbb} molecular states*

J. M. Dias[1,2;1)] Qi-Xin Yu(余圻昕)[1,3;2)] Wei-Hong Liang(梁伟红)[1,4;3)] Zhi-Feng Sun(孙志峰)[5]
Ju-Jun Xie(谢聚军)[6,7,8] E. Oset[1,9;4)]

[1]Department of Physics, Guangxi Normal University, Guilin 541004, China
[2]Instituto de Física, Universidade de São Paulo, Rua do Matão 1371. Butantã, CEP 05508-090, São Paulo, São Paulo, Brazil
[3]Institute for Experimental Physics, Department of Physics, University of Hamburg, Luruper Chaussee 149, D-22761 Hamburg, Germany
[4]Guangxi Key Laboratory of Nuclear Physics and Technology, Guangxi Normal University, Guilin 541004, China
[5]School of Physical Science and Technology, Lanzhou University, Lanzhou 730000, China
[6]Institute of Modern Physics, Chinese Academy of Sciences, Lanzhou 730000, China
[7]School of Physics and Microelectronics, Zhengzhou University, Zhengzhou 450001, China
[8]School of Nuclear Science and Technology, University of Chinese Academy of Sciences, Beijing 100049, China
[9]Departamento de Física Teórica and IFIC, Centro Mixto Universidad de Valencia-CSIC Institutos de Investigación de Paterna, Aptdo.22085, 46071 Valencia, Spain

Abstract: Using the vector exchange interaction in the local hidden gauge approach, which in the light quark sector generates the chiral Lagrangians and has produced realistic results for Ω_c, Ξ_c, Ξ_b and the hidden charm pentaquark states, we study the meson-baryon interactions in the coupled channels that lead to the Ξ_{bb} and Ω_{bbb} excited states of the molecular type. We obtain seven states of the Ξ_{bb} type with energies between 10408 and 10869 MeV, and one Ω_{bbb} state at 15212 MeV.

Keywords: doubly-heavy baryons , strong interaction, molecular state

DOI: 10.1088/1674-1137/44/6/064101

1 Introduction

Doubly- and triply-heavy baryons have attracted continuous theoretical attention [1-3] which has been intensified with the recent finding of the Ξ_{cc}^{++} state by LHCb [4]. Ξ_{bb} and Ω_{bbb} states have not yet been found, but are likely to be observed in the future by the LHCb or Belle II collaborations[5)]. Thus, it is appropriate to make theoretical predictions before the experiments are performed. Concerning the Ξ_{bb} and Ω_{bbb} states, most of the theoretical work concentrated on quark model calculations with three quarks. Pioneering work in this field was presented in Ref. [5]. A reference work on doubly- and triply-heavy baryons is Ref. [6]. More recently, there has been a theoretical revival stimulated by the new experimental findings and one finds studies of doubly-heavy baryons in Refs. [7-20], and of triply-heavy baryons in Refs. [10, 21-27], among others. Lattice QCD has also been used to make predictions of these states [28-30]. Calculations with pentaquark configurations are available in Refs. [31, 32]. Suggestions on how to observe these states by looking at weak decay products have been made in Refs. [33, 34], and using the e^+e^- colliders in Ref. [35]. Yet, molecular states of this type based on the meson-baryon interaction have not been investigated so far, and this is the purpose of the present work.

Molecular states bound by the meson-baryon strong interaction in coupled channels are peculiar. While there can be states bound by several tens of MeV, there are oth-

Received 25 December 2019 Published online 3 April 2020

* Partly supported by the National Natural Science Foundation of China (11975083, 11947413, 11847317, 11565007, 11735003, 1191101015). Q. X Yu acknowledges the support from the National Natural Science Foundation of China (11775024, 11575023, 11805153) and China Scholarship Council. Partly supported by the Spanish Ministerio de Economia y Competitividad and European FEDER funds (FIS2017- 84038-C2-1-P B, FIS2017-84038-C2-2-P B), and the Generalitat Valenciana in the program Prometeo II-2014/068, and the project Severo Ochoa of IFIC, SEV-2014-0398

1) E-mail: isengardjor@gmail.com
2) E-mail: yuqx@mail.bnu.edu.cn
3) E-mail: liangwh@gxnu.edu.cn
4) E-mail: oset@ific.uv.es

5) The effective efficiency for reconstruction of beauty hadrons is small, which makes the reconstruction of two beauty hadrons difficult. Yet, searches for such states are going on at LHCb, and such states should become more accessible in future updates of present facilities (Ivan Belyaev, private communication).

ers which are very close to the threshold of meson-baryon channels. Let's assume, to begin with, that we have just one meson-baryon channel bound by a small binding energy B. The coupling of this state to the meson-baryon component g is such that $-g^2 \left.\frac{\partial G}{\partial E}\right|_{E_B} = 1$ ($E_B$is the energy of the bound state), where G is the meson-baryon loop function such that the scattering matrix is given by $T = V + VGT$. This function has a cusp at the threshold of the meson-baryon channel, such that its derivative to the left is infinite at the threshold. Thus, $g^2 \to 0$ as the binding B goes to zero [36]. This can be derived from another perspective and is known as the Weinberg compositeness condition [37, 38], with $g^2 \sim \sqrt{B}$. What is less known is that if the bound state is close to the threshold of one of the coupled channels, then the couplings of the bound state to all channels reduce to zero [36, 39]. As a consequence, the decay widths for the channels, proportional to g_i^2, go to zero and one obtains automatically very narrow widths. This property, so naturally obtained with molecular states, is a source of permanent problems in the three-quark or tight pentaquark models of these states [40].

A clear situation favoring molecular states is the recent finding of three narrow pentaquark states by the LHCb collaboration close to the $\Sigma_c\bar{D}$, $\Sigma_c\bar{D}^*$ thresholds [41], which have been interpreted in a large number of papers as molecular states [42-56]. This is also the case in Ref. [57], where the earlier predictions made in Ref. [58] were updated. The same molecular model has been successful in predicting three of the five narrow Ω_c states found by LHCb [59] in Refs. [60-62], of some Ξ_c states reported in PDG [63], and of $\Xi_b(6227)$ observed by the LHCb collaboration [64] in Ref. [65]. Predictions of Ξ_{bc} states that have not yet observed were made in Ref. [66]. We should point out that the molecular picture is not the only one which claims to reproduce these states, and a variety of other models have been suggested. Abundant information can be found in a series of review papers [1-3, 67-78]. In this sense, making predictions with different models prior to experiments is useful to gain a better understanding of the nature of these states. Our work is written in this perspective.

We use here the same interaction that has been tested successfully in other cases and make predictions for the Ξ_{bb} and Ω_{bbb} states.

2 Formalism

In order to understand the classification of the meson-baryon states considered, it is convenient to begin with the interaction we use. Let us look, as an example, at the $B^-\Lambda_b \to B^-\Lambda_b$ transition shown in Fig. 1. By means of the mechanism of Fig. 1(b), one can exchange a $u\bar{u}$ state between B^- and Λ_b. This could physically correspond to a π, ρ or ω meson. One can equally exchange a $b\bar{b}$ pair which could correspond to η_b or Υ, but we can anticipate that η_b or Υ exchange, corresponding to a meson propagator, would be very much suppressed because of the large mass of the $b\bar{b}$ state compared to $u\bar{u}$.

We next consider the case where we have K^- instead of B^- in Fig. 1, where the chiral Lagrangians can be used to obtain the strength of the exchange mechanism. We recall the observation in Ref. [79] that the chiral Lagrangians can be obtained from the local hidden gauge Lagrangians which rely on the exchange of vector mesons [80-83]. In the $K^-\Lambda_b \to K^-\Lambda_b$ interaction, we have the $u\bar{u}$ exchange and the s quark as a spectator, the same as in the diagram Fig. 1(b) where the b quark is a spectator. We can make a mapping from the $K^-\Lambda_b \to K^-\Lambda_b$ interaction to the $B^-\Lambda_b \to B^-\Lambda_b$ interaction at the quark level, taking into account that when writing the S matrix at the meson level the normalization factors of the meson fields $\frac{1}{\sqrt{2E_K}}$, $\frac{1}{\sqrt{2E_B}}$ are different. These considerations were made in Ref. [84].

In the evaluation of the $B^-\Lambda_b \to B^-\Lambda_b$ transition in Fig. 1(b), instead of the Langrangians one can use the operators at the quark level, both in the upper vertex BBV [85] and in the lower vertex $\Lambda_b\Lambda_bV$, with V the exchanged vector meson [61], to get the same result. For practical reasons, we use the Lagrangian for the upper vertex

$$\mathcal{L} = -\mathrm{i}g\langle\left[P,\partial_\mu P\right]V^\mu\rangle, \tag{1}$$

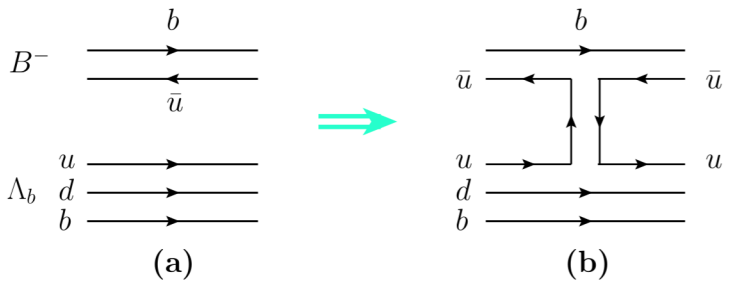

Fig. 1. (a) Quark representation of $B^-\Lambda_b$; (b) Meson exchange mechanism for the $B^-\Lambda_b \to B^-\Lambda_b$ transition.

where $\langle\cdots\rangle$ stands for the matrix trace, $g=\dfrac{M_V}{2f_\pi}$ ($M_V\sim 800$ MeV is the vector mass, $f_\pi=93$ MeV), and P, V are the $q\bar{q}$ matrices written in terms of pseudoscalar or vector mesons, with quarks u, d, s, b . Hence

$$P=\begin{pmatrix} \frac{1}{\sqrt{2}}\pi^0+\frac{1}{\sqrt{3}}\eta+\frac{1}{\sqrt{6}}\eta' & \pi^+ & K^+ & B^+ \\ \pi^- & -\frac{1}{\sqrt{2}}\pi^0+\frac{1}{\sqrt{3}}\eta+\frac{1}{\sqrt{6}}\eta' & K^0 & B^0 \\ K^- & \bar{K}^0 & -\frac{1}{\sqrt{3}}\eta+\sqrt{\frac{2}{3}}\eta' & B_s^0 \\ B^- & \bar{B}^0 & \bar{B}_s^0 & \eta_b \end{pmatrix}, \tag{2}$$

$$V=\begin{pmatrix} \frac{1}{\sqrt{2}}\rho^0+\frac{1}{\sqrt{2}}\omega & \rho^+ & K^{*+} & B^{*+} \\ \rho^- & -\frac{1}{\sqrt{2}}\rho^0+\frac{1}{\sqrt{2}}\omega & K^{*0} & B^{*0} \\ K^{*-} & \bar{K}^{*0} & \phi & B_s^{*0} \\ B^{*-} & \bar{B}^{*0} & \bar{B}_s^{*0} & \Upsilon \end{pmatrix}, \tag{3}$$

where we use the η-η' mixing of Ref. [86]. The lower vertex is of the type $V_\nu\gamma^\nu$, and we make the approximation that the momenta of the particles are small compared to their masses and $\gamma^\nu\to\gamma^0\equiv 1$, rendering the interaction spin independent. This means that after contraction of $V^\mu V^\nu$, only the ∂_0 component of ∂_μ in Eq. (1) is operative. The lower vertex is still evaluated at the quark level and the Lagrangian is trivial in terms of the operators,

$$L\to\begin{cases} \dfrac{g}{\sqrt{2}}(u\bar{u}-d\bar{d}), & \text{for } \rho^0 \\ \dfrac{g}{\sqrt{2}}(u\bar{u}+d\bar{d}), & \text{for } \omega \end{cases}, \tag{4}$$

which has to be sandwiched between the baryon wave functions. The next step to complete the program is to write the wave functions, and here we divert from using $SU(4)$ or other extensions of $SU(5)$, because the heavy quarks are not identical particles to the u, d, s quarks. We single out the heavy quark and impose the flavor-spin symmetry on the light quarks. If instead we have two or three b quarks, then we impose the flavor-spin symmetry on the b quarks. Once this is clarified, we have the following meson-baryon states with two b quarks:

1) bb in the baryon,

$$\Xi_{bb},\ \Omega_{bb},$$

and the meson-baryon states are

$$\pi\Xi_{bb},\quad \eta\Xi_{bb},\quad K\Omega_{bb}. \tag{5}$$

Since we have two identical b quarks, the spin wave function has to be symmetric in these quarks. We take them as number 1 and 2, and thus we must use the mixed symmetric spin wave function χ_{MS} for the first two quarks.

2) One b quark in the baryon and one in the meson. The meson-baryon states are

$$\bar{B}\Lambda_b,\quad \bar{B}\Sigma_b,\quad \bar{B}_s\Xi_b,\quad \bar{B}_s\Xi_b'. \tag{6}$$

In this case the flavor-spin symmetry is imposed on the second and third (light) quarks. The baryon states are classified as shown in Table 1.

We need $\chi_{MS}(12)$, $\chi_{MS}(23)$ and $\chi_{MA}(23)$, which are given in Ref. [87] for $s_3=\frac{1}{2}$,

$$\chi_{MS}(12)=\frac{1}{\sqrt{6}}(\uparrow\downarrow\uparrow+\downarrow\uparrow\uparrow-2\uparrow\uparrow\downarrow), \tag{7}$$

$$\chi_{MS}(23)=\frac{1}{\sqrt{6}}(\uparrow\uparrow\downarrow+\uparrow\downarrow\uparrow-2\downarrow\uparrow\uparrow), \tag{8}$$

$$\chi_{MA}(23)=\frac{1}{\sqrt{2}}(\uparrow\uparrow\downarrow-\uparrow\downarrow\uparrow). \tag{9}$$

Note that with our spin independent interaction, Ξ_{bb} and Ω_{bb} can have spin overlap with the other baryon components of Table 1, since

$$\langle\chi_{MS}(12)|\chi_{MS}(23)\rangle=-\frac{1}{2}, \tag{10}$$

$$\langle\chi_{MS}(12)|\chi_{MA}(23)\rangle=-\frac{\sqrt{3}}{2}. \tag{11}$$

We also consider vector-baryon states and pseudoscalar combinations with baryons with $J^P=\frac{3}{2}^+$, Ξ_{bb}^*, Ω_{bb}^*, Σ_b^*, Ξ_b^* , shown in Table 2. They all have the full symmetric spin wave function χ_S,

$$\chi_S(s_3=1)=\uparrow\uparrow\uparrow. \tag{12}$$

Table 1. Wave functions for baryons with $J^P=\frac{1}{2}^+$ and $I=0,\frac{1}{2},1$. MS and MA stand for mixed symmetric and mixed antisymmetric.

states	I,J	flavor	spin
Ξ_{bb}^0	$\frac{1}{2},\frac{1}{2}$	bbu	$\chi_{MS}(12)$
Ω_{bb}^-	$0,\frac{1}{2}$	bbs	$\chi_{MS}(12)$
Λ_b^0	$0,\frac{1}{2}$	$b\frac{1}{\sqrt{2}}(ud-du)$	$\chi_{MA}(23)$
Σ_b^0	$1,\frac{1}{2}$	$b\frac{1}{\sqrt{2}}(ud+du)$	$\chi_{MS}(23)$
Ξ_b^0	$\frac{1}{2},\frac{1}{2}$	$b\frac{1}{\sqrt{2}}(us-su)$	$\chi_{MA}(23)$
$\Xi_b'^0$	$\frac{1}{2},\frac{1}{2}$	$b\frac{1}{\sqrt{2}}(us+su)$	$\chi_{MS}(23)$

Table 2. Wave functions for baryons with $J^P=\frac{3}{2}^+$ and $I=0,\frac{1}{2},1$. S in χ_S stands for full symmetric.

states	I,J	Flavor	spin
Ξ_{bb}^{*0}	$\frac{1}{2},\frac{3}{2}$	bbu	χ_S
Ω_{bb}^{*-}	$0,\frac{3}{2}$	bbs	χ_S
Σ_b^{*0}	$1,\frac{3}{2}$	$b\frac{1}{\sqrt{2}}(ud+du)$	χ_S
Ξ_b^{*0}	$\frac{1}{2},\frac{3}{2}$	$b\frac{1}{\sqrt{2}}(us+su)$	χ_S

The combination of vector-baryon ($\frac{3}{2}^+$) gives rise to states in a region difficult to identify experimentally [57] and we do not study them.

In the case of vector-baryon interaction, the upper vertex is evaluated using Eq. (1) by substituting $\left[P,\partial_\mu P\right]$ with $\left[V_\nu,\partial_\mu V^\nu\right]$. In the limit of small momenta, V^μ of Eq. (1) is the exchanged vector. Hence, the interaction is calculated in the same way as for pseudoscalars except that there is an extra $\vec{\epsilon}\cdot\vec{\epsilon}\,'$ factor which gives the spin independence of the upper vertex [61]. Therefore, the interaction is spin independent. This feature allows to classify the channels into different blocks:

a) $\pi\Xi_{bb}$, $\eta\Xi_{bb}$ and $K\Omega_{bb}$ with $\chi_{MS}(12)$, $\bar{B}\Lambda_b$ and $\bar{B}_s\Xi_b$ with $\chi_{MA}(23)$;

b) $\pi\Xi_{bb}$, $\eta\Xi_{bb}$ and $K\Omega_{bb}$ with $\chi_{MS}(12)$, $\bar{B}\Sigma_b$ and $\bar{B}_s\Xi'_b$ with $\chi_{MS}(23)$;

c) $\rho\Xi_{bb}$, $\omega\Xi_{bb}$, $\phi\Xi_{bb}$ and $K^*\Omega_{bb}$ with $\chi_{MS}(12)$, $\bar{B}^*\Lambda_b$ and $\bar{B}^*_s\Xi_b$ with $\chi_{MA}(23)$;

d) $\rho\Xi_{bb}$, $\omega\Xi_{bb}$, $\phi\Xi_{bb}$ and $K^*\Omega_{bb}$ with $\chi_{MS}(12)$, $\bar{B}^*\Sigma_b$ and $\bar{B}^*_s\Xi'_b$ with $\chi_{MS}(23)$;

e) $\pi\Xi^*_{bb}$, $\eta\Xi^*_{bb}$, $K\Omega^*_{bb}$, $\bar{B}\Sigma^*_b$ and $\bar{B}_s\Xi^*_b$ with all states in χ_S.

Taking into account our isospin phase convention $(-\pi^+,\pi^0,\pi^-)$, (B^+,B^0), $(\bar{B}^0,-B^-)$, (K^+,K^0) and $(\bar{K}^0,-K^-)$, we can construct the isospin wave function for the blocks to have isospin $I=\frac{1}{2}$ for the global "Ξ_{bb}" states. Using the vector-exchange interaction discussed above, we obtain a potential V_{ij} for the $i\to j$ transition of the type

$$V_{ij}=D_{ij}\frac{1}{4f_\pi^2}(k^0+k'^0), \tag{13}$$

where, k^0, k'^0 are the meson energies in channel i and channel j, respectively, and D_{ij} are the coefficients which are given in the tables below.

Note that since $\chi_{MS}(12)$ in the Ξ_{bb}, Ω_{bb} states overlaps with $\chi_{MS}(23)$ and $\chi_{MA}(23)$, blocks a) and b) can mix and have to be put together. The same can be said for blocks c) and d), which also have to be put together. We then obtain the D_{ij} coefficients shown in Tables 4, 6, 8 (note that we changed the order of baryon-meson in the tables, which must be taken into account when constructing the isospin wave functions). In Tables 3, 5, 7 we show the thresholds of the channels considered. The masses which are not tabulated in PDG [63] are taken from Refs. [13, 88]. In the tables there are terms which go with parameter λ. They correspond to transitions that require B^* exchange. Because of the large mass of B^* compared to the light vectors, these terms are very much suppressed. With the same considerations as in Ref. [61], we estimate λ as

$$\lambda=\frac{-m_V^2}{(m_B-m_\eta)^2-m_{B^*}^2}\approx 0.1. \tag{14}$$

We note that when the light vector mesons are exchanged, the heavy quarks are spectators, and hence these terms automatically fulfill the rules of heavy quark symmetry. The exchange of B^* makes the b quark active. This term goes barely as $O(\frac{1}{m_Q})$ (with m_Q the heavy quark mass) and is not subject to the heavy quark spin symmetry rules. Note that these terms are very small in our approach, as expected.

We turn now to the Ω_{bbb} states. Here, the coupled channels are $\eta\Omega_{bbb}$, $\bar{B}\Xi^*_{bb}$, $\bar{B}_s\Omega^*_{bb}$. The baryon states involved are tabulated in Table 9. The $\eta\Omega_{bbb}$, $\bar{B}\Xi^*_{bb}$, $\bar{B}_s\Omega^*_{bb}$

Table 3. Pseudoscalar-baryon($\frac{1}{2}^+$) (PB) channels considered for the sector with $J^P=\frac{1}{2}^-$.

channel	$\Xi_{bb}\pi$	$\Xi_{bb}\eta$	$\Omega_{bb}K$	$\Lambda_b\bar{B}$	$\Sigma_b\bar{B}$	$\Xi_b\bar{B}_s$	$\Xi'_b\bar{B}_s$
threshold/MeV	10335	10745	10756	10899	11092	11160	11302

Table 4. D_{ij} coefficients for the PB sector with $J^P=\frac{1}{2}^-$.

$J^P=\frac{1}{2}^-$	$\Xi_{bb}\pi$	$\Xi_{bb}\eta$	$\Omega_{bb}K$	$\Lambda_b\bar{B}$	$\Sigma_b\bar{B}$	$\Xi_b\bar{B}_s$	$\Xi'_b\bar{B}_s$
$\Xi_{bb}\pi$	-2	0	$\sqrt{\frac{3}{2}}$	$\frac{3}{4}\lambda$	$-\frac{1}{4}\lambda$	0	0
$\Xi_{bb}\eta$		0	$-\frac{2}{\sqrt{3}}$	$\frac{1}{2\sqrt{2}}\lambda$	$\frac{1}{2\sqrt{2}}\lambda$	$-\frac{1}{2\sqrt{2}}\lambda$	$\frac{1}{2\sqrt{6}}\lambda$
$\Omega_{bb}K$			-1	0	0	$-\sqrt{\frac{3}{8}}\lambda$	$-\frac{1}{2\sqrt{2}}\lambda$
$\Lambda_b\bar{B}$				-1	0	-1	0
$\Sigma_b\bar{B}$					-3	0	$\sqrt{3}$
$\Xi_b\bar{B}_s$						-1	0
$\Xi'_b\bar{B}_s$							-1

Table 5. Vector-baryon($\frac{1}{2}^+$) (VB) channels considered for the sector with $J^P=\frac{1}{2}^-,\frac{3}{2}^-$.

channel	$\Lambda_b\bar{B}^*$	$\Xi_{bb}\rho$	$\Xi_{bb}\omega$	$\Sigma_b\bar{B}^*$	$\Omega_{bb}K^*$	$\Xi_b\bar{B}^*_s$	$\Xi_{bb}\phi$	$\Xi'_b\bar{B}^*_s$
threshold/MeV	10945	10972	10980	11138	11156	11208	11216	11350

Table 6. D_{ij} coefficients for the VB sector with $J^P = \frac{1}{2}^-, \frac{3}{2}^-$.

$J^P = \frac{1}{2}^-, \frac{3}{2}^-$	$\Lambda_b \bar{B}^*$	$\Xi_{bb}\rho$	$\Xi_{bb}\omega$	$\Sigma_b \bar{B}^*$	$\Omega_{bb} K^*$	$\Xi_b \bar{B}_s^*$	$\Xi_{bb}\phi$	$\Xi_b' \bar{B}_s^*$
$\Lambda_b \bar{B}^*$	-1	$\frac{3}{4}\lambda$	$\frac{\sqrt{3}}{4}\lambda$	0	0	-1	0	0
$\Xi_{bb}\rho$		-2	0	$-\frac{1}{4}\lambda$	$\sqrt{\frac{3}{2}}$	0	0	0
$\Xi_{bb}\omega$			0	$\frac{\sqrt{3}}{4}\lambda$	$-\frac{1}{\sqrt{2}}$	0	0	0
$\Sigma_b \bar{B}^*$				-3	0	0	0	$\sqrt{3}$
$\Omega_{bb} K^*$					-1	$\frac{1}{\sqrt{2}}\lambda$	1	$-\frac{1}{2\sqrt{2}}\lambda$
$\Xi_b \bar{B}_s^*$						-1	$\sqrt{\frac{3}{8}}\lambda$	0
$\Xi_{bb}\phi$							0	$-\frac{1}{2\sqrt{2}}\lambda$
$\Xi_b' \bar{B}_s^*$								-1

Table 7. Pseudoscalar-baryon($\frac{3}{2}^+$) (PB) channels considered for the sector with $J^P = \frac{3}{2}^-$.

channel	$\Xi_{bb}^* \pi$	$\Xi_{bb}^* \eta$	$\Omega_{bb}^* K$	$\Sigma_b^* \bar{B}$	$\Xi_b^* \bar{B}_s$
threshold/MeV	10374	10784	10793	11113	11320

Table 8. D_{ij} coefficients for the PB sector with $J^P = \frac{3}{2}^-$.

$J^P = \frac{3}{2}^-$	$\Xi_{bb}^*\pi$	$\Xi_{bb}^*\eta$	$\Omega_{bb}^* K$	$\Sigma_b^* \bar{B}$	$\Xi_b^* \bar{B}_s$
$\Xi_{bb}^*\pi$	-2	0	$\sqrt{\frac{3}{2}}$	$\frac{1}{2}\lambda$	0
$\Xi_{bb}^*\eta$		0	$-\frac{2}{\sqrt{3}}$	$-\frac{1}{\sqrt{2}}\lambda$	$-\frac{1}{\sqrt{6}}\lambda$
$\Omega_{bb}^* K$			-1	0	$\frac{1}{\sqrt{2}}\lambda$
$\Sigma_b^* \bar{B}$				-3	$\sqrt{3}$
$\Xi_b^* \bar{B}_s$					-1

Table 9. Wave functions of baryons with $J^P = \frac{3}{2}^+$ and $I = 0, \frac{1}{2}$.

states	I, J	flavor	spin
Ω_{bbb}^-	$0, \frac{3}{2}$	bbb	χ_S
Ξ_{bb}^{*0}	$\frac{1}{2}, \frac{3}{2}$	bbu	χ_S
Ω_{bb}^{*-}	$0, \frac{3}{2}$	bbs	χ_S

channels with $J^P = \frac{3}{2}^-$, do not couple with the "Ξ_{bb}" states since they contain one more b quark. In Table 10, we show the threshold masses of the pseudoscalar-baryon channels, and in Table 11 the D_{ij} coefficients.

Table 10. PB channels considered for the sector with $J^P = \frac{3}{2}^-$ and three b quarks.

channel	$\Omega_{bbb}\eta$	$\Xi_{bb}^* \bar{B}$	$\Omega_{bb}^* \bar{B}_s$
threshold/MeV	15382	15515	15664

Table 11. D_{ij} coefficients for the PB sector with $J^P = \frac{3}{2}^-$ and three b quarks.

$J^P = \frac{3}{2}^-$	$\Omega_{bbb}\eta$	$\Xi_{bb}^* \bar{B}$	$\Omega_{bb}^* \bar{B}_s$
$\Omega_{bbb}\eta$	0	$-\frac{2}{\sqrt{6}}\lambda$	$-\frac{1}{\sqrt{3}}\lambda$
$\Xi_{bb}^* \bar{B}$		-2	$\sqrt{2}$
$\Omega_{bb}^* \bar{B}_s$			-1

3 Results

With the V_{ij} potential of Eq. (13), we solve the Bethe-Salpeter equation in coupled channels

$$T = [1 - VG]^{-1} V, \tag{15}$$

where G is the diagonal meson-baryon loop function given by

$$\begin{aligned} G_l =& \mathrm{i}\int \frac{\mathrm{d}^4 q}{(2\pi)^4} \frac{M_l}{E_l(\vec{q})} \frac{1}{k^0 + p^0 - q^0 - E_l(\vec{q}) + \mathrm{i}\epsilon} \frac{1}{q^2 - m_l^2 + \mathrm{i}\epsilon} \\ =& \int_{|\vec{q}|<q_{\max}} \frac{\mathrm{d}^3 q}{(2\pi)^3} \frac{1}{2\omega_l(\vec{q})} \frac{M_l}{E_l(\vec{q})} \frac{1}{k^0 + p^0 - \omega_l(\vec{q}) - E_l(\vec{q}) + \mathrm{i}\epsilon}, \end{aligned} \tag{16}$$

with p^0 the energy of the incoming baryon in the meson-baryon rest frame. m_l and M_l are the meson and baryon masses, and ω_l and E_l their energies $\omega_l = \sqrt{m_l^2 + \vec{q}^{\,2}}$ and $E_l = \sqrt{M_l^2 + \vec{q}^{\,2}}$. As in the studies [61, 85, 89], we use a three-momentum cut-off $q_{\max} = 650$ MeV to regularize the loop function. The poles are searched for on the second Riemann sheet, as done in Refs. [61, 85, 89], and the couplings of the states to the different channels are obtained from the residues of the T_{ij} matrix at the pole z_R, knowing that close to the pole one has

$$T_{ij}(s) = \frac{g_i g_j}{\sqrt{s} - z_R}. \tag{17}$$

The second Riemann sheet is obtained using $G^{II}(s)$ instead of $G(s)$ given by

$$G_l^{II} = \begin{cases} G_l(s), & \text{for } \mathrm{Re}(\sqrt{s}) < \sqrt{s}_{\mathrm{th},l} \\ G_l(s) + \mathrm{i}\dfrac{2M_l q}{4\pi\sqrt{s}}, & \text{for } \mathrm{Re}(\sqrt{s}) \geqslant \sqrt{s}_{\mathrm{th},l} \end{cases}, \tag{18}$$

where $\sqrt{s}_{\mathrm{th},l}$ is the threshold mass of the l-th channel, and

$$q = \frac{\lambda^{1/2}(s, m_l^2, M_l^2)}{2\sqrt{s}}, \quad \text{with } \mathrm{Im}(q) > 0. \tag{19}$$

In Tables 12 and 13, we show the couplings and the wave function at the origin for two states with $J^P = \frac{1}{2}^-$ obtained from the coupled channels of Table 4. In addi-

tion to the couplings g_i, we show the values of $g_i G_i^{II}$ at the pole, which according to Ref. [36] provide the strength of the wave function at the origin.

We find two states, one at 10408 MeV with a width of about 186 MeV , which couples mostly to the $\Xi_{bb}\pi$ component, with a non-negligible coupling to $\Omega_{bb}K$ and $\Lambda_b\bar{B}$. The large width of this state stems from the large coupling to the $\Xi_{bb}\pi$ channel and the fact that this channel is open. The second state appears at 10686 MeV with a very small width. It couples mostly to the $\Sigma_b\bar{B}$ channel, which is closed. The $\Xi_{bb}\pi$ channel is open, but the coupling to this channel is very small, which justifies the small width obtained.

Some of the components are quite bound and one may think that these components should be very small. Yet, this is not the case, since, as shown in detail in Ref. [66] the size of the channels is not linked to the binding but is determined by the cut-off, and $r^2|\psi(r)|^2$ peaks around $r = 0.7$ fm, with still a significant strength around 1 fm.

We now consider the states generated from the coupled channels of Table 6 from vector-baryon ($\frac{1}{2}^+$) states. We find three states with zero width, degenerate in $J^P = \frac{1}{2}^-, \frac{3}{2}^-$. We note that the additional pion exchange would break this degeneracy but, as discussed in Ref. [66], its effects are largely incorporated in our approach with a suitable choice of $q_{\rm max}$, and only a small part remains and produces a small splitting between the $\frac{1}{2}^-$ and $\frac{3}{2}^-$ states. The small difference between the masses of the hidden charm pentaquark states $P_c(4440)$ and $P_c(4452)$ of Ref. [41], assumed to be $\frac{1}{2}^-, \frac{3}{2}^-$, respectively, corroborates this finding.

In Tables 14, 15 and 16, we show the properties of these three states. The first state appears at 10732 MeV and couples mostly to $\Sigma_b\bar{B}^*$, the second is at 10807 MeV and couples mostly to $\Lambda_b\bar{B}^*$, while the third appears at 10869 MeV and couples mostly to $\Xi_{bb}\rho$. Note that all channels are closed which is why we obtain zero widths.

Let us look at the states formed from the pseudoscalar-baryon ($\frac{3}{2}^+$) channels of Table 8. We find two states, shown in Tables 17 and 18. The first appears at 10447 MeV with a width of about 186 MeV. This state couples mostly to $\Xi^*_{bb}\pi$, which is open, justifying the large width. The second state appears at 10707 MeV and couples mostly to $\Sigma^*_b\bar{B}$. The $\Xi^*_{bb}\pi$ channel is open, but the small coupling to this channel results in a very small width of this state.

Finally, we consider the only " Ω_{bbb}" state found from the coupled channels of Table 10. This state is at 15212 MeV and couples mostly to $\Xi^*_{bb}\bar{B}$, as shown in Table 19. All coupled channels are closed and we obtain a zero width for this state.

In summary, we obtained two excited Ξ_{bb} states with

Table 12. The g_i couplings of the 10408.18 + i93.18 state (generated dynamically in the PB sector with $J^P = \frac{1}{2}^-$) to various channels and $g_i G_t^{II}$ (in MeV).

10408.18+i93.18	$\Xi_{bb}\pi$	$\Xi_{bb}\eta$	$\Omega_{bb}K$	$\Lambda_b\bar{B}$	$\Sigma_b\bar{B}$	$\Xi_b\bar{B}_s$	$\Xi'_b\bar{B}_s$
g_i	1.69 + i1.21	−0.02 − i0.09	−0.86 − i0.73	−1.03 − i0.31	0.50 + i0.23	−0.28 − i0.19	−0.16 − i0.12
$g_i G_i^{II}$	−73.58 − i12.87	0.01 + i0.58	4.52 + i5.41	0.79 + i0.39	−0.29 − i0.18	0.14 + i0.12	0.07 + i0.06

Table 13. The g_i couplings of the 10686.39 + i0.08 state (generated dynamically in the PB sector with $J^P = \frac{1}{2}^-$) to various channels and $g_i G_i^{II}$ (in MeV).

10686.39+i0.08	$\Xi_{bb}\pi$	$\Xi_{bb}\eta$	$\Omega_{bb}K$	$\Lambda_b\bar{B}$	$\Sigma_b\bar{B}$	$\Xi_b\bar{B}_s$	$\Xi'_b\bar{B}_s$
g_i	0.01 − i0.05	−0.10 + i0.02	−0.05 + i0.04	0.06 + i0.02	19.03	0.02 + i0.02	−10.80
$g_i G_i^{II}$	1.57 + i0.51	1.52 − i0.23	0.72 − i0.52	−0.11 − i0.03	−18.78	−0.02 − i0.02	7.23

Table 14. The g_i couplings of the 10732.01 + i0 state (generated dynamically in the VB sector with $J^P = \frac{1}{2}^-, \frac{3}{2}^-$) to various channels and $g_i G_i^{II}$ (in MeV).

10732.01+i0	$\Lambda_b\bar{B}^*$	$\Xi_{bb}\rho$	$\Xi_{bb}\omega$	$\Sigma_b\bar{B}^*$	$\Omega_{bb}K^*$	$\Xi_b\bar{B}^*_s$	$\Xi_{bb}\phi$	$\Xi'_b\bar{B}^*_s$
g_i	−0.01	0.15	−0.14	19.13	−0.10	0	−0.03	−10.86
$g_i G_t^{II}$	0.02	−1.01	0.88	−18.72	0.42	0	0.09	7.18

Table 15. The g_i couplings of the 10807.41 + i0 state (generated dynamically in the VB sector with $J^P = \frac{1}{2}^-, \frac{3}{2}^-$) to various channels and $g_i G_i^{II}$ (in MeV).

10807.41+i0	$\Lambda_b\bar{B}^*$	$\Xi_{bb}\rho$	$\Xi_{bb}\omega$	$\Sigma_b\bar{B}^*$	$\Omega_{bb}K^*$	$\Xi_b\bar{B}^*_s$	$\Xi_{bb}\phi$	$\Xi'_b\bar{B}^*_s$
g_i	7.82	−0.66	−0.12	0.06	0.16	7.57	−0.10	−0.04
$g_i G_t^{II}$	−18.77	5.52	0.97	−0.07	−0.76	−7.37	0.39	0.03

Table 16. The g_i couplings of the 10869.63 + i0 state (generated dynamically in the VB sector with $J^P = \frac{1}{2}^-, \frac{3}{2}^-$) to various channels and $g_i G_i^{II}$ (in MeV).

10869.63+i0	$\Lambda_b \bar{B}^*$	$\Xi_{bb}\rho$	$\Xi_{bb}\omega$	$\Sigma_b \bar{B}^*$	$\Omega_{bb} K^*$	$\Xi_b \bar{B}_s^*$	$\Xi_{bb}\phi$	$\Xi_b' \bar{B}_s^*$
g_i	0.61	3.57	−0.36	−0.37	−2.41	1.18	0.48	0.26
$g_i G_i^{II}$	−2.25	−38.50	3.76	0.53	13.34	−1.34	−2.16	−0.21

Table 17. The g_i couplings of the 10447.50 + i93.31 state (generated dynamically in the PB($\frac{3}{2}^+$) sector with $J^P = \frac{3}{2}^-$) to various channels and $g_i G_i^{II}$ (in MeV).

10447.50+i93.31	$\Xi_{bb}^* \pi$	$\Xi_{bb}^* \eta$	$\Omega_{bb}^* K$	$\Sigma_b^* \bar{B}$	$\Xi_b^* \bar{B}_s$
g_i	1.69 + i1.21	−0.03 − i0.10	−0.87 − i0.73	−1.03 − i0.49	0.34 + i0.26
$g_i G_i^{II}$	−73.61 − i12.82	0.05 + i0.62	4.58 + i5.47	0.60 + i0.39	0.15 − i0.14

Table 18. The g_i couplings of the 10706.87 + i0.30 state (generated dynamically in the PB($\frac{3}{2}^+$) sector with $J^P = \frac{3}{2}^-$) to various channels and $g_i G_i^{II}$ (in MeV).

10706.87+i0.30	$\Xi_{bb}^* \pi$	$\Xi_{bb}^* \eta$	$\Omega_{bb}^* K$	$\Sigma_b^* \bar{B}$	$\Xi_b^* \bar{B}_s$
g_i	−0.01 + i0.09	0.19 − i0.03	0.08 − i0.07	19.01 − i0.01	−10.79 + i0.01
$g_i G_i^{II}$	−3.04 − i1.20	−2.55 + i0.35	−1.06 + i0.91	−18.75 − i0.01	7.25 + i0.01

Table 19. The g_i couplings of the 15212.04 + i0 state (generated dynamically in the PB($\frac{3}{2}^+$) sector with $J^P = \frac{3}{2}^-$ and three b quarks) to various channels and $g_i G_i^{II}$ (in MeV).

15212.04+i0	$\Omega_{bbb}\eta$	$\Xi_{bb}^* \bar{B}$	$\Omega_{bb}^* \bar{B}_s$
g_i	0.15	14.03	−9.82
$g_i G_i^{II}$	−1.44	−18.31	8.80

$J^P = \frac{1}{2}^-$ coupled to the pseudoscalar-baryon ($\frac{1}{2}^+$) channels, three states with $J^P = \frac{1}{2}^-, \frac{3}{2}^-$, degenerate in our approach, coupled to the vector-baryon ($\frac{1}{2}^+$) channels, two states with $J^P = \frac{3}{2}^-$ coupled to the pseudoscalar-baryon ($\frac{3}{2}^+$) channels, and found only one state corresponding to an excited Ω_{bbb} state, coupled to the pseudoscalar-baryon ($\frac{3}{2}^+$) channels.

We used the mass of the Ω_{bbb} ground state from Ref. [13], 14834 MeV. This is quite different from the Lattice QCD calculations in Ref. [29], 14371 MeV, similar to Ref. [6]. Surprisingly, if we redo the calculations using this latter mass, we obtain a mass of the excited Ω_{bbb} state of Table 19 which differs by less than 1 MeV from the former. The reason is that the obtained excited Ω_{bbb} state is mostly a $\Xi_{bb}^* \bar{B}$ molecule and the $\Omega_{bbb}\eta$ channel plays a negligible role. This is due to the zero D_{ii} coefficient for $\Omega_{bbb}\eta$ in Table 11, which indicates that there is no direct interaction in this channel. The negligible effect of this channel in the excited Ω_{bbb} state can also be seen in the small coupling to this channel, 0.15 versus 14.03 for the coupling to the $\Xi_{bb}^* \bar{B}$ channel. The latter channel is bound by about 300 MeV, which again is due to the scale of the masses and the large $D_{ii} = -2$ coefficient for the diagonal $\Xi_{bb}^* \bar{B} \to \Xi_{bb}^* \bar{B}$ transition.

4 Conclusions

We carried out a study of the interactions of meson-baryon coupled channels that lead to the formation of bound or resonant states, corresponding to the excited Ξ_{bb} and Ω_{bbb} states. As in related studies of Ξ_c, Ξ_b, Ξ_{bc} and hidden charm molecular states, we used an interaction based on the exchange of vector mesons, which in the case of light quarks gives rise to the chiral Lagrangians. In particular, the exchange of light vectors, which produces the dominant part of the interaction, leaves the heavy quarks as spectators and fulfills the rules of heavy quark symmetry. We find seven Ξ_{bb} states and one Ω_{bbb} state of molecular nature. The success in describing the hidden charm pentaquark states, and of some Ω_c, Ξ_c, Ξ_b states using the same input for the interaction, supports our confidence that the predictions are realistic. It will be interesting to compare them with the future measurements which are likely to be made by LHCb and Belle II.

We thank the Guangxi Normal University for hospitality, where the main part of this work was done.

References

1 S. L. Olsen, T. Skwarnicki, and D. Zieminska, Rev. Mod. Phys., **90**(1): 015003 (2018)

2 M. Karliner, J. L. Rosner, and T. Skwarnicki, Ann. Rev. Nucl. Part. Sci., **68**: 17 (2018)

3 Y. R. Liu, H. X. Chen, W. Chen *et al.*, Prog. Part. Nucl. Phys., **107**: 237 (2019)
4 R. Aaij *et al.* (LHCb Collaboration), Phys. Rev. Lett., **119**(11): 112001 (2017)
5 A. De Rujula, H. Georgi, and S. L. Glashow, Phys. Rev. D, **12**: 147 (1975)
6 B. Silvestre-Brac, Few Body Syst., **20**: 1 (1996)
7 T. D. Cohen and P. M. Hohler, Phys. Rev. D, **74**: 094003 (2006)
8 Q. X. Yu and X. H. Guo, Nucl. Phys. B, **947**: 114727 (2019)
9 J. M. Flynn, E. Hernandez, and J. Nieves, Phys. Rev. D, **85**: 014012 (2012)
10 X. Z. Weng, X. L. Chen, and W. Z. Deng, Phys. Rev. D, **97**(5): 054008 (2018)
11 Z. Shah and A. K. Rai, Eur. Phys. J. C, **77**(2): 129 (2017)
12 D. Ebert, R. N. Faustov, V. O. Galkin *et al.*, Phys. Rev. D, **66**: 014008 (2002)
13 W. Roberts and M. Pervin, Int. J. Mod. Phys. A, **23**: 2817 (2008)
14 A. Valcarce, H. Garcilazo, and J. Vijande, Eur. Phys. J. A, **37**: 217 (2008)
15 M. Karliner and J. L. Rosner, Phys. Rev. D, **90**(9): 094007 (2014)
16 L. Y. Xiao, Q. F. Lü, and S. L. Zhu, Phys. Rev. D, **97**(7): 074005 (2018)
17 L. Meng, H. S. Li, Z. W. Liu *et al.*, Eur. Phys. J. C, **77**(12): 869 (2017)
18 R. Dutta and A. Bhol, Phys. Rev. D, **96**(7): 076001 (2017)
19 T. M. Aliev and S. Bilmis, Nucl. Phys. A, **984**: 99 (2019)
20 M. Karliner and J. L. Rosner, Phys. Rev. D, **97**(9): 094006 (2018)
21 J. Vijande, A. Valcarce, and H. Garcilazo, Phys. Rev. D, **91**(5): 054011 (2015)
22 K. W. Wei, B. Chen, N. Liu *et al.*, Phys. Rev. D, **95**(11): 116005 (2017)
23 Z. Shah and A. K. Rai, Eur. Phys. J. A, **53**(10): 195 (2017)
24 G. Yang, J. Ping, P. G. Ortega *et al.*, Chin. Phys. C, **44**: 023102 (2020)
25 Z. Shah and A. K. Rai, Few Body Syst., **59**(5): 76 (2018)
26 M. Radin, S. Babaghodrat, and M. Monemzadeh, Phys. Rev. D, **90**(4): 047701 (2014)
27 T. M. Aliev, K. Azizi, and M. Savcl, J. Phys. G, **41**: 065003 (2014)
28 S. Meinel, Phys. Rev. D, **85**: 114510 (2012)
29 S. Meinel, Phys. Rev. D, **82**: 114514 (2010)
30 M. Padmanath, R. G. Edwards, N. Mathur *et al.*, Phys. Rev. D, **90**(7): 074504 (2014)
31 Q. S. Zhou, K. Chen, X. Liu *et al.*, Phys. Rev. C, **98**(4): 045204 (2018)
32 S. Y. Li, Y. R. Liu, Y. N. Liu *et al.*, Eur. Phys. J. C, **79**(1): 87 (2019)
33 Y. J. Shi, W. Wang, Y. Xing *et al.*, Eur. Phys. J. C, **78**(1): 56 (2018)
34 W. Wang and J. Xu, Phys. Rev. D, **97**(9): 093007 (2018)
35 X. C. Zheng, C. H. Chang, and Z. Pan, Phys. Rev. D, **93**(3): 034019 (2016)
36 D. Gamermann, J. Nieves, E. Oset *et al.*, Phys. Rev. D, **81**: 014029 (2010)
37 S. Weinberg, Phys. Rev., **137**: B672 (1965)
38 V. Baru, J. Haidenbauer, C. Hanhart *et al.*, Phys. Lett. B, **586**: 53 (2004)
39 H. Toki, C. Garcia-Recio, and J. Nieves, Phys. Rev. D, **77**: 034001 (2008)
40 A. Pilloni, talk at the MIAPP Workshop, Munchen, October 2019. http://www.munich-iapp.de/programmes-topical-workshops/2019/hadron-spectroscopy/daily-schedule-neu/?L=%2Fproc%2Fse
41 R. Aaij *et al.* (LHCb Collaboration), Phys. Rev. Lett., **122**(22): 222001 (2019)
42 H. X. Chen, W. Chen, and S. L. Zhu, Phys. Rev. D, **100**(5): 051501 (2019)
43 M. Z. Liu, Y. W. Pan, F. Z. Peng *et al.*, Phys. Rev. Lett., **122**(24): 242001 (2019)
44 J. He, Eur. Phys. J. C, **79**(5): 393 (2019)
45 R. Chen, Z. F. Sun, X. Liu *et al.*, Phys. Rev. D, **100**(1): 011502 (2019)
46 J. R. Zhang, Eur. Phys. J. C, **79**(12): 1001 (2019)
47 L. Meng, B. Wang, G. J. Wang *et al.*, Phys. Rev. D, **100**(1): 014031 (2019)
48 M. B. Voloshin, Phys. Rev. D, **100**(3): 034020 (2019)
49 Y. Yamaguchi, H. Garcia-Tecocoatzi, A. Giachino *et al.*, arXiv: 1907.04684[hep-ph].
50 Z. G. Wang and X. Wang, arXiv: 1907.04582[hep-ph].
51 M. Pavon Valderrama, Phys. Rev. D, **100**(9): 094028 (2019)
52 Y. J. Xu, C. Y. Cui, Y. L. Liu *et al.*, arXiv: 1907.05097[hep-ph].
53 M. Z. Liu, T. W. Wu, M. Sanchez Sanchez *et al.*, arXiv: 1907.06093[hep-ph].
54 T. J. Burns and E. S. Swanson, Phys. Rev. D, **100**(11): 114033 (2019), arXiv:1908.03528[hep-ph]
55 Y. H. Lin and B. S. Zou, Phys. Rev. D, **100**(5): 056005 (2019)
56 Y. Yamaguchi, A. Hosaka, S. Takeuchi *et al.*, arXiv: 1908.08790[hep-ph].
57 C. W. Xiao, J. Nieves, and E. Oset, Phys. Rev. D, **100**(1): 014021 (2019)
58 J. J. Wu, R. Molina, E. Oset *et al.*, Phys. Rev. Lett., **105**: 232001 (2010)
59 R. Aaij *et al.* (LHCb Collaboration), Phys. Rev. Lett., **118**(18): 182001 (2017)
60 G. Montana, A. Feijoo, and A. Ramos, Eur. Phys. J. A, **54**(4): 64 (2018)
61 V. R. Debastiani, J. M. Dias, W. H. Liang *et al.*, Phys. Rev. D, **97**(9): 094035 (2018)
62 J. Nieves, R. Pavao, and L. Tolos, Eur. Phys. J. C, **78**(2): 114 (2018)
63 M. Tanabashi *et al.* (Particle Data Group), Phys. Rev. D, **98**(3): 030001 (2018)
64 R. Aaij *et al.* (LHCb Collaboration), Phys. Rev. Lett., **121**(7): 072002 (2018)
65 Q. X. Yu, R. Pavao, V. R. Debastiani *et al.*, Eur. Phys. J. C, **79**(2): 167 (2019)
66 Q. X. Yu, J. M. Dias, W. H. Liang *et al.*, Eur. Phys. J. C, **79**(12): 1025 (2019)
67 H. X. Chen, W. Chen, X. Liu *et al.*, Phys. Rept., **639**: 1 (2016)
68 H. X. Chen, W. Chen, X. Liu *et al.*, Rept. Prog. Phys., **80**(7): 076201 (2017)
69 A. Esposito, A. Pilloni, and A. D. Polosa, Phys. Rept., **668**: 1 (2017)
70 A. Hosaka, T. Iijima, K. Miyabayashi *et al.*, PTEP, **2016**(6): 062C01 (2016)
71 J. M. Richard, Few Body Syst., **57**(12): 1185 (2016)
72 R. F. Lebed, R. E. Mitchell, and E. S. Swanson, Prog. Part. Nucl. Phys., **93**: 143 (2017)
73 Y. Dong, A. Faessler, and V. E. Lyubovitskij, Prog. Part. Nucl. Phys., **94**: 282 (2017)
74 F. K. Guo, C. Hanhart, U. G. Meißner *et al.*, Rev. Mod. Phys., **90**(1): 015004 (2018)
75 A. Ali, J. S. Lange, and S. Stone, Prog. Part. Nucl. Phys., **97**: 123 (2017)
76 E. Kou *et al.* (Belle-II Collaboration), PTEP, **12**: 123C01 (2019)
77 Y. S. Kalashnikova and A. V. Nefediev, Phys. Usp., **62**(6): 568 (2019)
78 N. Brambilla, S. Eidelman, C. Hanhart *et al.*, arXiv: 1907.07583[hep-ex]
79 G. Ecker, J. Gasser, H. Leutwyler *et al.*, Phys. Lett. B, **223**: 425 (1989)
80 M. Bando, T. Kugo, S. Uehara *et al.*, Phys. Rev. Lett., **54**: 1215 (1985)
81 M. Bando, T. Kugo, and K. Yamawaki, Phys. Rept., **164**: 217 (1988)
82 U. G. Meißner, Phys. Rept., **161**: 213 (1988)
83 H. Nagahiro, L. Roca, A. Hosaka *et al.*, Phys. Rev. D, **79**: 014015 (2009)
84 W. H. Liang, C. W. Xiao, and E. Oset, Phys. Rev. D, **89**(5): 054023 (2014)
85 S. Sakai, L. Roca, and E. Oset, Phys. Rev. D, **96**(5): 054023 (2017)
86 A. Bramon, A. Grau, and G. Pancheri, Phys. Lett. B, **283**: 416 (1992)
87 F. E. Close, "An Introduction to Quarks and Partons", Academic Press, Cambrige, 1979
88 C. Albertus, E. Hernandez, J. Nieves *et al.*, Eur. Phys. J. A **32**, 183(2007), Erratum: [Eur. Phys. J. A **36**, 119(2008)]
89 J. M. Dias, V. R. Debastiani, J.-J. Xie *et al.*, Phys. Rev. D, **98**(9): 094017 (2018)